APMC 2023
5-8 DEC @TICC, Taipei, TAIWAN
Taiwan Microwave Association/Chang Gung University

2023 Asia-Pacific Microwave Conference

Dec. 5 - 8, 2023@TAIWAN

Microwave Linking the World

Dec. 8, Friday	10:10-11:50
FR-A2 **(Room 201A)**	**Control Circuits (Mixer, Oscillator, Switch, etc.) (II)** **Chairs:** Jia-Shiang Fu (National Central University, Taiwan), Da-Chiang Chang (Taiwan Semiconductor Research Institute, Taiwan)
	220152: A Synchronized 35 GHz Divide-by-5 TSPC Flip-Flop Clock Divider in 22 nm FDSOI Florian Probst, Andre Engelmann and Robert Weigel (Friedrich-Alexander-Universität Erlangen-Nürnberg, Germany) ***220202: A 25–50 GHz Inductor-Less Divide-by-4 with Microstrip Line Connection in 40 nm CMOS*** Sho Okii, Yohtaro Umeda and Kyoya Takano (Tokyo University of Science, Japan) Shinsuke Hara, Satoru Tanoi and Akifumi Kasamatsu (National Institute of Information and Communications Technology, Japan) ***220487: Low Phase Noise DDS-Driven PLL Frequency Synthesizer for Joint Communication and Sensing Applications*** Zhiqiang Liu (Purple Mountain Laboratories, China) Haiyang Xia and Lianming Li (Southeast University & Purple Mountain Laboratories, China) Lin Lu and Xuan Wang (Southeast University, China) Chenhui Xia (The 58th Research Institute of China Electronics Technology Group, China) ***220534: A 27-39 GHz Fractional-N PLL For 5G mm-Wave Communication With Improved Extended Range Multi-Modulus Divider*** Kai Sun, Lin Lu, Shutao Ye and Xiangning Fan (Southeast University, China) Junliang Wang (Nanjing University of Science and Technology, China) Lianming Li (Southeast University, Purple Mountain Laboratory National Mobile Communications Research Laboratory, China)
FR-B2 **(Room 201B)**	**Filters and Resonators** **Chairs:** Kamran Ghorbani (RMIT University, Australia), Cristiano Tomassoni (University of Perugia, Italy)
	220444: UHF Bandpass Filter Using a Combination of Semi-Lumped and Lumped Components Amir Ebrahimi and Kamran Ghorbani (RMIT University, Australia) ***220280: Compact 3-D Printed Rectangular Waveguide Diplexer With Wide Stopband Response*** Abdul Rehman and Cristiano Tomassoni (University of Perugia, Italy) ***220097: Ultra-Compact Substrate Integrated Waveguide Bandpass Filter with Unequal Termination Impedance*** Phanam Pech, Samdy Saron, Girdhari Chaudhary and Yongchae Jeong (Jeonbuk National University, Korea) ***220141: Quasi-Elliptic Bandpass Filter With Controllable Multiple Transmission Zeros Using Coupled Lines*** Girdhari Chaudhary, Phanam Pech, Samdy Saron and Yongchae Jeong (Jeonbuk National University, Korea) ***220214**: **A Compact W-band Diplexer for Integration with an Electronically Steerable Focal Plane Array Antenna System*** Sohaib Yaqoob Chaudhry, Viktor Chernikov, Artem Vilenskiy and Marianna Ivashina(Chalmers University of Technology, Sweden), Sam Agneessens and Lars Manholm(Ericsson Research,

Quasi-Elliptic Bandpass Filter With Controllable Multiple Transmission Zeros Using Coupled Lines

Girdhari Chaudhary
JIANT-IT Human Resource Development Center
Jeonbuk National University
Jeonju-si, South Korea
girdharic@jbnu.ac.kr

Phanam Pech
Division of Electronic and Informating Engineering
Jeonbuk National University
Jeonju-si, South Korea
pechphanam@jbnu.ac.kr

Samdy Saron
Division of Electronic and Information Engineering
Jeonbuk National University
Jeonju-si, South Korea
saronsamdy@jbnu.ac.kr

Yongchae Jeong
Division of Electronic Engineering
Jeonbuk National University
Jeonju-si, South Korea
ycjeong@jbnu.ac.kr

***Abstract*—This paper presents RF design methodology for quasi-elliptic bandpass filter (BPF) with multiple transmission zeros (TZs). The proposed filter consists of a coupled line BPF section and TZ sections. Both sections comprised of coupled lines with short-circuit stubs. By generating multiple TZs at lower and upper sides of the passband, a quasi-elliptic BPF response can be achieved without affecting the passband response. For experimental proof of concept, a prototype of microstrip line quasi-elliptic BPF was designed and manufactured at center frequency of 3.5 GHz. The measured results demonstrate good agreement with EM simulations and theoretically predicted outcomes.**

Keywords—Bandpass filter (BPF), coupled lines, group delay, multiple transmission zeros, quasi-elliptic response.

I. Introduction

Planar bandpass filters (BPFs) with high performance characteristics, including low insertion loss, sharp skirt, and high frequency selectivity, are essential for effectively utilizing the limited and precious electromagnetic spectrum in wireless applications. One way to enhance the filtering selectivity in BPFs is by an increasing filter order. However, this approach results in higher insertion loss and a larger circuit size. As a result, an effective alternative approach for achieving high selectivity is the use of quasi-elliptic BPF with a finite number of transmission zeros (TZs). Previous research has explored various approaches for designing quasi-elliptic BPF. These approaches include cross-coupling between nonadjacent resonators [1], mixed electric and magnetic coupling [2], and extracted pole synthesis [3]. Coupled lines have been found wide application in the design of various types of BPFs. In [4], a high selectivity BPF with multiple TZs is described, utilizing three pairs of quarter-wavelength coupled lines and two pairs of half-wavelength series transmission lines. Similarly, work [5] presents a quasi-elliptic BPF with two TZs using open circuited and short-circuited coupled lines. However, this particular structure is limited to generating two symmetrical TZs.

In this work, we present a simple design method for a quasi-elliptic BPF with multiple TZs. The proposed approach utilizes a pair of coupled lines with short-circuited stubs to achieve desired passband characteristics. The multiple number of symmetrical TZs are generated near to passband, thereby enhancing the selectivity characteristics of the quasi-elliptic BPF. For experimental validation, quasi-elliptic BPF with two TZs is designed, fabricated, and measured.

II. Design Theory

Fig. 1 illustrates the circuit schematic of the proposed quasi-elliptic BPF with multiple TZs. The filter structure consists of BPF section and two TZ sections (TZ section A and B). The BPF section is a designed as 3-pole BPF, consisting of two coupled lines and short-circuited stubs. Similarly, each TZ section comprises a set of coupled lines with a short-circuited TL. For simplicity, all characteristic impedances of coupled lines (z_{0ei}, z_{0oi}) and TLs (z_t, z_1, z_2) are normalized to Z_0 = 50 Ω. The electrical length of coupled lines and TLs are equal to $\theta = \lambda/4$ at center frequency (f_0).

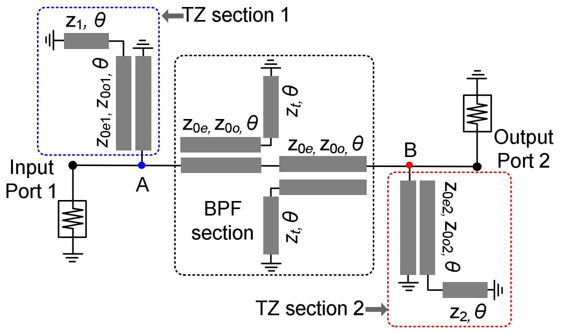

Fig. 1. Proposed structure of quasi-elliptic BPF using coupled lines.

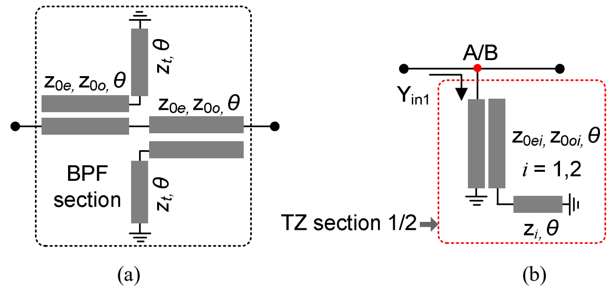

Fig. 2. (a) Proposed structure of 3-pole coupled line BPF and (b) TZ sections.

A. BPF section design using group delay analysis approach

Fig. 2(a) illustrates the 3-pole BPF section utilizing a coupled line and short-circuited stubs. Conventionally, a parallel coupled line BPF needs *N*+1 number of coupled lines (*N*: number of filter order), resulting in a large physical size. However, in this work, we propose a 3-pole BPF section that employs only two coupled lines and short-circuited stubs instead of four coupled lines. Assuming coupling coefficient k_i is a free design variable, normalized even-mode impedance z_{0e} is expressed in terms of k and odd-mode admittance z_{0o} as (1).

$$z_{0e} = \frac{1+k}{1-k} z_{0o} \tag{1}$$

The group delay analysis approach has been employed to determine circuit parameters of the proposed 3-pole BPF section [6]. By equating the group delay of the proposed BPF section with that of a conventional 3-pole BPF, the solution of z_{0o} can be found as (2).

$$z_{0o}=\frac{(1-k)\sqrt{z_t^2+z_t m\left(1-z_t mk^2\right)}-z_t(1-k)}{1-z_t mk^2}, \qquad (2)$$

where

$$m=1+\frac{2g_1+g_2}{\pi\Delta}+\frac{(g_1+2g_2)\pi\Delta}{4g_1g_2} \qquad (3)$$

and g_i is low-pass prototype element values and Δ is a fractional bandwidth of 3-pole BPF. From (2) and (3), it is worth noting that z_{0o} can be obtained by providing the values of k, z_t, and Δ. Once z_{0o} is determined, the value of z_{0e} can be obtained using (1).

Fig. 3 illustrates the simulated frequency response of BPF section. In this design example, the low pass filter (LPF) prototypes are chosen for Chebyshev response with passband ripple of 0.1 dB. As shown in Fig. 3, the proposed BPF section provides 3-pole BPF response by utilizing only two coupled lines and short-circuited shunt stubs. The bandwidth of BPF can be controlled by appropriately selecting values of z_t and k of coupled lines. Increasing the coefficient results in the wider bandwidth for BPF section.

B. Transmission zeros section

Fig. 2(b) shows the TZ section which consists of a coupled line (z_{0ei}, z_{0oi}) and a short-circuited TL with characteristic impedance of z_i and electrical length θ. The TZ section does not affect the passband of BPF since the input admittance Y_{in1} at point A or B will be equal to zero at f_0. However, at certain frequencies other than f_0, input admittance becomes infinite (Z_{in1} = 1/Y_{in1} = 0). As a result, the TZs are generated at lower and upper sides of passband. The frequency of TZs can be specified using equation (4).

$$f_{TZ}^{i}=\frac{2f_0}{\pi}\cos^{-1}\left\{\pm\sqrt{\frac{z_i\left(z_{0ei}^2-2z_{0ei}z_{0oi}+z_{0oi}^2\right)}{\left(z_{0ei}+z_{0oi}\right)\left\{2z_{0ei}z_{0oi}+z_i\left(z_{0ei}+z_{0oi}\right)\right\}}}\right\} \qquad (4)$$

As observed from (4), each TZ section generates two symmetrical TZs. It should be noted that if the circuit parameters of both TZ section (TZ section A and B) are different, four TZs can be generated near to passband. These TZs contribute to the enhancement of the selectivity of BPF without affecting the passband response.

Fig. 4 shows the simulated transmission magnitude ($|S_{21}|$) of TZ section. From the results, it is evident that TZs frequencies at lower and upper stopbands can be adjusted by selecting the appropriate values of z_{0ei}, z_{0oi}, and z_i, without affecting the passband response. When even- and odd-mode impedances of coupled lines are fixed value, changing value of z_i from 0.6 Ω to 2.4 Ω causes the TZs to shift away from passband. Similarly, if z_i is fixed, TZs location can be controlled by adjusting values of z_{0ei} and z_{0oi}.

C. Design Examples of Quasi-elliptic BPF

Fig. 5 shows the simulated frequency response of the overall circuit of the proposed quasi-elliptic BPF. The circuit parameters of the quasi-elliptic BPF are shown in Table I.

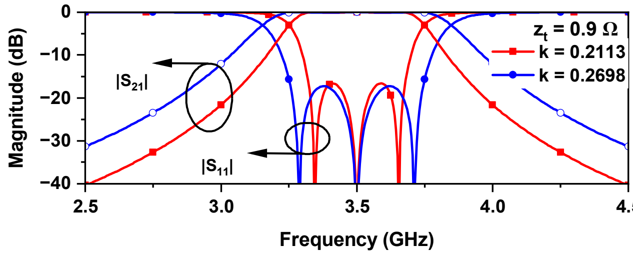

Fig. 3. *S*-parameters results of BPF section with different coupling coefficient (k) of coupled lines.

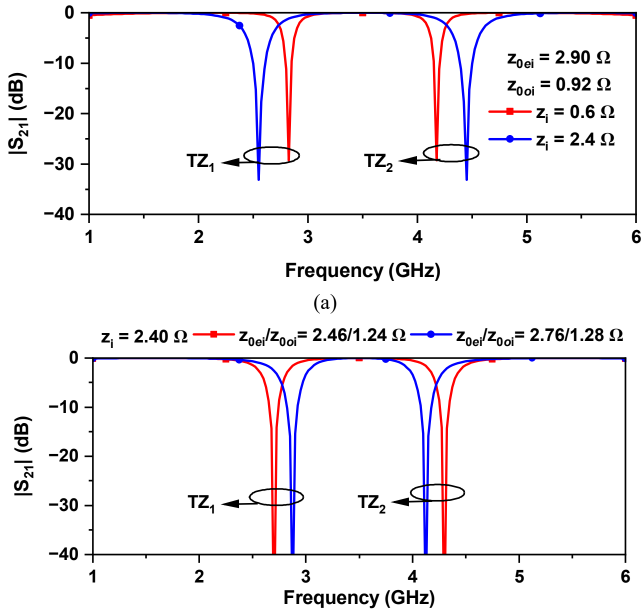

(a) (b)

Fig. 4. Transmission zero (TZ) control for different (a) z_1 and (b) z_{0e1}/z_{0o1}.

Table I. Circuit parameters of quasi-elliptic BPF

Example	$z_{0e}/z_{0o}/z_t$ (Ω)	$z_{0e1}/z_{0o1}/z_1$ (Ω)	$z_{0e2}/z_{0o2}/z_2$ Ω)
1	2.60/1.22/0.68	2.6/0.8/2.40	
2	2.62/1.24/0.68	2.9/0.92/0.7	
3	2.60/1.22/0.68	2.60/0.846/0.6	2.60/0.8/2.4

From simulation results, it is evident that multiple TZs can be generated in close to the passband. In design examples 1 and 2, TZ sections have same parameter values, resulting only two symmetrical pair of TZs as depicted in Fig. 5(a) and 5(b). Location of these symmetrical TZs can be moved closer to passband by selecting low characteristics impedance (z_1 = z_2) of short-circuited stub. On the other hand, in design example 3, the circuit parameters of TZ section A and B are different. As result, four TZs are generated, as shown in Fig. 5(c). The presence of multiple TZs contributes to the improvement of the frequency selectivity of the proposed BPF.

III. Experimental Results

To validate the proposed design, a prototype of the quasi-elliptic BPF with two TZs is designed and fabricated at f_0 = 3.5 GHz. The prototype was implemented using a Taconic substrate with dielectric constant of 2.20 and thickness of 0.787 mm. The design goal was to achieve quasi-elliptic BPF response with TZs located at 2.90 GHz and 4.10 GHz. The circuit parameters of the designed quasi-elliptic BPF are given as follows: z_{0e} = 2.52 Ω, z_{0o} = 1.35 Ω, z_t = 0.7 Ω, z_{0e1} = z_{0e1}= 3.12 Ω, z_{0o1} = z_{0o2} =1.40 Ω, z_1 = z_2 = 1.68 Ω. The circuit parameters are normalized to 50 Ω.

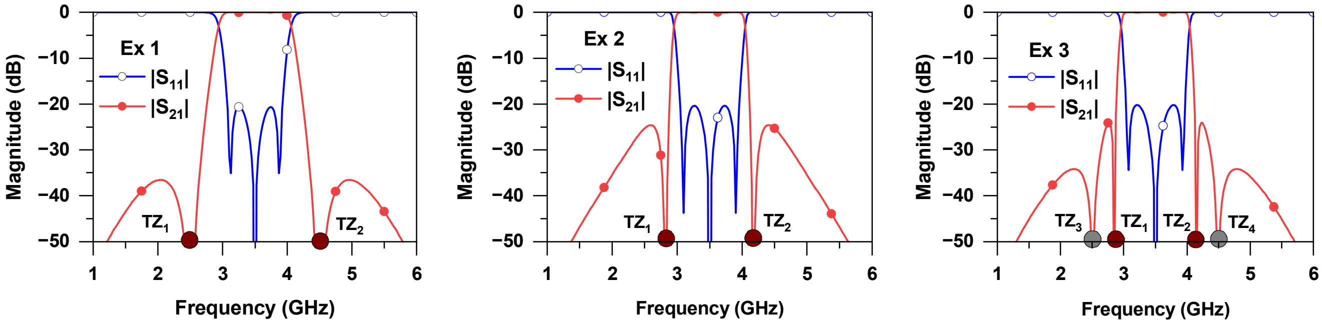

Fig. 5. *S*-parameters of BPF section results in Fig. (2a) with different coupling coefficient (*k*) of the coupled lines.

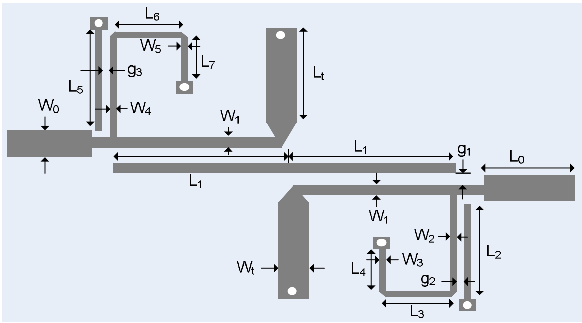

(a)

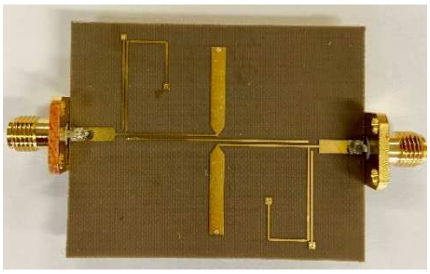

(b)

Fig. 6. (a) Physical layout of fabricated quasi-elliptic BPF with physical dimensions and (b) photograph of fabricated filter. Physical dimensions: W_0 = 2.40, $W_1 = W_2 = W_3 = W_4 = W_5 = 0.4$, $W_t = 2.6$, $g_1 = 0.42$, $g_2 = g_3 = 0.2$, $L_1 = 16$, $L_2 = L_5 = 15.8$, $L_3 = L_6 = 6$, $L_4 = L_7 = 5.9$, $L_0 = 4$, and $L_t = 13.92$. Dimensions unit: millimeter (mm).

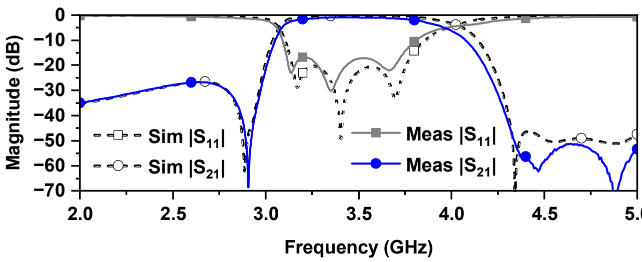

Fig. 7. Simulated and measured results of fabricated quasi-elliptic BPF.

Fig. 6(a) shows the physical layout of the fabricated quasi-elliptic BPF, including dimensions, which were optimized using ANSYS HFSS 2023. Fig. 6(b) shows the photograph of fabricated quasi-elliptic BPF.

Fig. 7 shows the comparison between the simulated and measured results of the fabricated quasi-elliptic BPF. The measured results are well agreed with EM simulation results. From the measured results, it can be observed that the proposed quasi-elliptic BPF exhibits three reflection poles in passband. The 3-dB bandwidth of filter is measured to be 820 MHz (23.42%) extending from 3.080 to 3.962 GHz. The measured insertion loss is 1.02 dB at f_0 = 3.50 GHz, while input and output return losses are higher than 16.78 dB within passband. The TZs are located at a lower stopband frequency of 2.90 GHz and higher stopband frequency of 4.46 GHz. Notably, the stopband attenuation exceeds 26.5 dB within in frequency range from DC to 2.96 GHz and from 4.25 GHz to 5 GHz.

IV. Conclusion

This paper presents a simple design approach for a quasi-elliptic BPF with multiple transmission zeros using coupled lines. By utilizing the proposed approach, it becomes possible to generate multiple transmission zeros at lower and higher stopband frequencies, thereby achieving high frequency selective characteristics. The locations of transmission zeros are controlled by adjusting circuit parameters of transmission zero section while ensuring the desired passband response is maintained. To validate the proposed design concept, a quasi-elliptic BPF with two transmission zeros is designed and fabricated at center frequency of 3.50 GHz. The measured results of fabricated prototype demonstrate good with simulations results.

Acknowledgment

This research was supported by National Research Foundation of Korea (NRF) grant funded by Korea Government (MSIT) (No. RS-2023-00209081) and in part by the Basic Science Research Program through the NRF grant funded by Ministry of Education (No. 2019R1A6A1A09031717).

References

[1] C. Chen, Y. Chen, and C. Chang, "Miniaturized microstrip cross-coupled filters using quarter-wave or quasi-quarter-wave resonators," *IEEE Trans. Microw. Theory Techn.*, vol. 51, no. 1, pp. 120–131, Jan. 2003.

[2] S. Zhang, L. Zhu, and R. Weerasekera, "Synthesis of inline mixed coupled quasi-elliptic bandpass filters based on $\lambda/4$ resonators," *IEEE Trans. Microw. Theory Techn.*, vol. 63, no. 10, pp. 3487–3493, Oct. 2015.

[3] K. S. K. Yeo and M. J. Lancaster, "The design of microstrip six-pole quasi-elliptic filter with linear phase response using extracted-pole technique," *IEEE Trans. Microw. Theory Techn.*, vol. 49, no. 2, pp. 321–327, Feb. 2001.

[4] K. Xu, D. Li and Y. Liu, "High-Selectivity wideband bandpass filter using simple coupled lines with multiple transmission poles and zeros," *IEEE Microwave and Wireless Components Letters*, vol. 29, no. 2, pp. 107-109, Feb. 2019.

[5] C. Chen, "A coupled-line coupling structure for the design of quasi-elliptic bandpass filters," *IEEE Transactions on Microwave Theory and Techniques*, vol. 66, no. 4, pp. 1921-1925, Apr. 2018.

[6] J. Lee, G. Chaudhary, P. Pech, and Y. Jeong, "A Design of 3-pole Coupled Line Bandpass Filter Using Group Delay Analysis Approach", *2022 International Symposium on Antennas and Propagation (ISAP)*, pp.111-112, 2022.